Inorganic Chemistry
Cite This: Inorg. Chem. 2019, 58, 12689−12699
Article
pubs.acs.org/IC

CNS and CNP Iron(II) Mono-Iron Hydrogenase (Hmd) Mimics: Role of Deprotonated Methylene(acyl) and the *trans*-Acyl Site in H_2 Heterolysis

Yae In Cho, Gummadi Durgaprasad, and Michael J. Rose*

Department of Chemistry, The University of Texas at Austin, Austin, Texas 78712, United States

Supporting Information

ABSTRACT: We report syntheses and H_2 activation involving model complexes of mono-iron hydrogenase (Hmd) derived from acyl-containing pincer ligand precursors bearing thioether (**CNS**^{Pre}) or phosphine (**CNP**^{Pre}) donor sets. Both complexes feature pseudo-octahedral iron(II) dicarbonyl units. While the **CNS** pincer adopts the expected *mer*-CNS (pincer) geometry, the **CNP** ligand unexpectedly adopts the *fac*-CNP coordination geometry. Both complexes exhibit surprisingly acidic methylene C−H bond (reversibly de/protonated by a bulky phenolate), which affords a putative dearomatized pyridinate-bound intermediate. Such base treatment of **Fe-CNS** also results in deligation of the thioether sulfur donor, generating an open coordination site *trans* from the acyl unit. In contrast, **Fe-CNP** maintains a CO ligand *trans* from the acyl site both in the parent and dearomatized complexes (the $-PPh_2$ donor is *cis* to acyl). The dearomatized *mer*-**Fe-CNS** was competent for H_2 activation (5 atm $D_{2(g)}$ plus phenolate as base), which is attributed to both the basic site on the ligand framework and the open coordination site *trans* to the acyl donor. In contrast, the dearomatized *fac*-**Fe-CNP** was *not competent* for H_2 activation, which is ascribed to the blocked coordination site *trans* from acyl (occupied by CO ligand). These results highlight the importance of both (i) the open coordination site *trans* to the organometallic acyl donor and (ii) a pendant base in the enzyme active site.

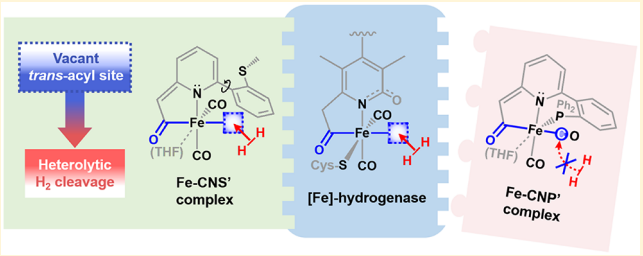

INTRODUCTION

In nature, dihydrogen activation has been accomplished by a class of enzymes called hydrogenases.[1] Among the three types, mono [Fe]-hydrogenase (Hmd) catalyzes the reversible cleavage of H_2 in a *nonredox*, heterolytic fashion as a key step during the methanogenic conversion of carbon dioxide (CO_2) to methane (CH_4).[2] In this process, the substrate methenyltetrahydromethanopterin (methenyl-H_4MPT^+) is used as a C_1 "carrier" throughout the metabolic pathway. As a result of H_2 activation by Hmd, a hydride is transferred to the H_4MPT^+ substrate, thus producing methylenetetrahydromethanopterin (methylene-H_4MPT) and a proton.[3,4]

The active site is composed of the following moieties (Scheme 1): a redox-inactive Fe(II) center, a bidentate acyl-pyridine moiety presenting N (pyridone/pyridinol) and C (acyl) donors derived from the so-called FeGP cofactor; an S donor from Cys176; *cis* carbonyl ligands; and last a labile/open coordination site (*trans* to acyl-C) for solvent or substrate binding.[2,5−7] As structure dictates function, close examination of particular coordination motifs through a biomimetic approach can aid in clarifying the role of each ligand and its orientation, thus providing deeper insight for understanding the catalytic mechanism.

One of the most intriguing features of [Fe]-hydrogenase is the presence of the Fe-acyl moiety. Indeed, this organometallic motif is thus far unique in biological systems. Electronically, the acyl-C donor cannot be replicated by any of the standard amino acid residues, nor by any of the ligands found in other hydrogenase enzymes (CO, CN^-, thiolate, azadithiolate, etc.). While it is an extremely strong σ-donor ($pK_a \approx 35$)—stronger than almost any other known biological ligand other than methyl ($pK_a \approx 45$; *e.g.* methylcobalimin)—it is also a good π-acceptor due to the available resonance form of the oxyanion/Fischer carbene (Fe=C−O$^-$). It is thus presumed to play a very specific role in the nonredox activation of H_2 and hydride transfer mechanism.

Regarding the geometry of the donors about the metal center, it can be reasonably postulated that in the absence of

Scheme 1. Active site of [Fe]-hydrogenase

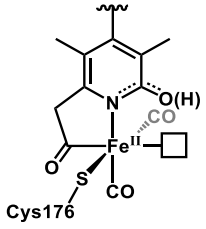

Received: May 23, 2019
Published: September 9, 2019

DOI: 10.1021/acs.inorgchem.9b01530
Inorg. Chem. 2019, 58, 12689−12699

Scheme 2. Structures of the Ligand Precursors (CNS^{Pre} and CNP^{Pre}), Our Previous Fe-carbamoyl Complex,[36] and the Fe-acyl Complexes (Fe-CNS and Fe-CNP) Used in This Work

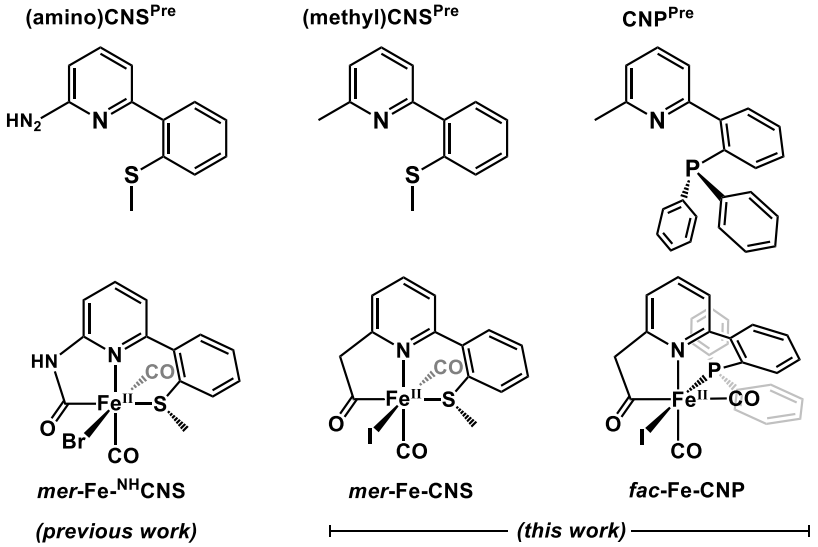

steric (or otherwise geometrically directing) effects, the strong σ-donating ability of the acyl-C directs the open/solvent binding site to its *trans* position. Indeed, this postulate is epitomized in the model chemistry developed by Hu, Pickett, and others—wherein non-macrocyclic CNS donor sets (i.e., the thiolate is not tethered to the acylpyridine or carbamoylpyridine moiety) inherently adopt a *fac*-CNS donor geometry with the solvent[8] or open[9−11] site *trans* from the acyl-C donor. However, reactivity studies with such "nontethered" model complexes have not been forthcoming, possibly due to the instability of hydride intermediates or lack of H_2 activation due to fluxional geometries. The strong *trans* influence of the acyl group (much stronger than carbonyl)[12] likely plays a major role in the catalysis in terms of electronic effects. In this respect, it is remarkable that nature chose to make use of a rare type of ligand to promote catalysis.

Metal−ligand cooperativity in small molecule systems, and even more broadly in active site chemistry,[13−16] has been recently noted. A number of related iron(II) carbonyl complexes have been investigated by organometallic and catalysis researchers in the past decade to better understand the role of each donor moiety. Milstein and co-workers adopted the use of pincer-type P^CN^CN and P^CN^CP-type ligands, in which the central pyridine presents two phosphine moieties at the *ortho* positions via methylene linkers.[17−20] A variety of Fe(II)−(PNN/PNP)−hydride complexes were shown to serve as hydrogenation catalysts, and—mechanistically—these species universally proceed through a dearomatized pyridinate species, wherein one of the picolinic protons in the methylene linker is deprotonated. Subsequently, the metal−ligand cooperativity of the Lewis acidic (metal) and basic (ligand) sites drive the heterolytic activation of H_2. In related work, Kirchner and co-workers focused on iron(II) complexes with P^NN^NP-type ligands where the pyridine ring and the phosphine moieties are connected by amide (NH) linkers instead.[21−23] Upon activation with strong base (NH deprotonation), the complexes catalyze the hydrogenation of ketones and aldehydes and proceed through the same heterolytic cleavage of H_2 as supported by DFT calculations.[21,23] Huang and co-workers[24−26] studies a number of ruthenium−PNN complexes that proceeded through the similarly "dearomatized" intermediate, and these Ru-pincer complexes catalyzed dehydrogenative couplings,[24] transfer hydrogenation,[25] and electrocatalytic reduction of CO_2.[26]

Among bioinorganic researchers, the Song group utilized 2-acylmethyl-6-pyridinol (or hydroxymethyl) ligands to chelate iron(II) and provide more structural resemblance to the [Fe]-hydrogenase enzyme active site.[27−29] Although lacking reactivity studies, they successfully implemented all the donor atoms in correct geometry and donor orientation as found in the active site. The Hu group has also investigated small-molecule mimics featuring acylmethylpyridine ligands exhibiting a 2-hydroxy,[11] 2-methoxy,[9,30] or 2-tertbutyl group;[11] a thiolate ligand (2,6-dimethylbenzenethiolate[9,11] and others);[11] and the *cis*-carbonyl motif. Through pioneering studies using a hybrid protein|molecule approach,[31] it was hypothesized that the following components are crucial in the H_2 activation: (i) the presence of a protein environment and substrate (methenyl-H_4MPT^+), (ii) thiolate ligand as an internal base (in other words, a proton acceptor), and (iii) the pyridine-2-OH moiety (or conjugate pyridone), which positions the active site/cofactor suitable for the heterolytic cleavage of H_2. The hybrid enzyme exhibited measurable reactivity (TOF = 2 and 1 s^{-1} for the heterolytic cleavage of H_2 in the presence of the substrate and the production of H_2, respectively),[31] which corresponded to about 1% of wild-type activity, thus exceeding the rates of the previously reported synthetic hydrogenation catalysts (TOF $\approx 10^{-3}$−10^{-1} s^{-1}).[32,33]

A recent study by our group demonstrated that preservation of the facial coordination motif of the CNS donors via an "anthracene scaffold" approach, a synthetic model can promote H_2 activation in the absence of the protein environment.[34] The active solvato-Fe(II) species not only activates H_2, but also abstracts hydride from a model imidazolidine substrate (hydride source via C−H activation), then produces H_2 with the aid of a bulky phenol (proton source). Furthermore, we recently demonstrated that functional H_2 activation and hydride transfer can be performed by a thiolate-containing model complex derived from this anthracene scaffold.[35]

More closely related to the present work, we reported the carbamoyl-pincer model complex $[(C^{NH}NS)Fe(CO)_2(Br)]$[36] (Scheme 2)—the carbamoyl version of the methylene-acyl **Fe-**

DOI: 10.1021/acs.inorgchem.9b01530
Inorg. Chem. 2019, 58, 12689−12699

Scheme 3. Metalation of CNS^{Pre} and CNP^{Pre} Ligand Precursors into the Acylmethylpyridyl-Fe(II) Complexes, Fe-CNS and Fe-CNP, Respectively

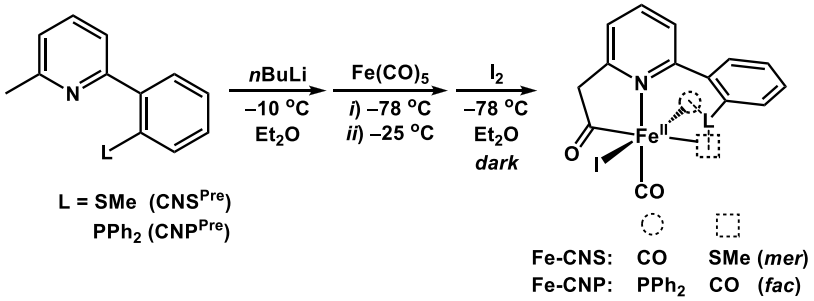

CNS complex in this report. The CNS donor set was ligated in standard pincer (meridional) fashion, and treatment with a hydride source ($NaHBEt_3$) provided spectroscopic evidence for the Fe−H species (low temp ^{1}H NMR spectroscopy: −5.08 ppm in d^8-THF). *However, the complex was not competent for H_2 activation*, and ligand decomposition was observed upon treatment with strong base (NH deprotonation). We were thus interested to determine the importance of the donor identity (acyl versus carbamoyl) in an analogous complex for H_2 activation.

In this work, we focus on the structural and reactivity effects of the methylene-acyl donor in concert with thioether versus phosphine donors in a single-chelate approach by reporting the new compounds, ligand precursor, CNS^{Pre}, and the iron(II)−acyl complexes, **Fe-CNS** and **Fe-CNP**. (CNP^{Pre} was synthesized previously:[37] here, we report a new synthetic route and use it as a ligand precursor for synthesizing acyl complex, **Fe-CNP**.). The apparent flexibility of this ligand frame allows the metal center to "choose" its ideal binding mode based on steric and electronic effects. The structures and enzyme-like reactivities of the resulting **Fe-CNS** and **Fe-CNP** complexes are compared herein in the "forward" direction, using D_2 activation in the presence or absence of base.

RESULTS

Syntheses. Metalations to prepare the **Fe-CNS** and **Fe-CNP** complexes were performed in analogous fashion (Scheme 3). As reported previously, syntheses of the acylmethylpyridyl−Fe(II) complexes typically proceed through (i) metalation of ligand (or ligand precursor) with Fe(0) or Fe(2−) carbonyls; (ii) migratory insertion of one of the carbonyls to generate the Fe(0) intermediate with the methylene−acyl−iron unit; finally, (iii) oxidation using X_2 (X = I or Br) to afford the desired Fe(II)−acyl complex.[12,27] When using Fe(0) carbonyls (as in this work), a harsh deprotonation of the methylpyridine moiety of a chosen ligand precursor is required prior to the metalation step. The crude product was collected as a yellow−brown powder, and purification via alumina chromatography provided analytically pure and crystallographically defined samples.

Crystal Structures: Reasons for *mer* versus *fac* Coordination Motifs. The crystal structures of the Fe−acyl thioether (**Fe-CNS**) and phosphine (**Fe-CNP**) complexes are depicted in Figure 1. In each case, the Fe(II) center is coordinated with one iodide, two carbonyls, and one ligand (C, N, and L donors). Notably, the ligation mode of the "pincer" ligand is different in each complex: **Fe-CNS** exhibits meridional binding, whereas **Fe-CNP** exhibits an unexpected facial coordination motif. In each case, one CO ligand occupies

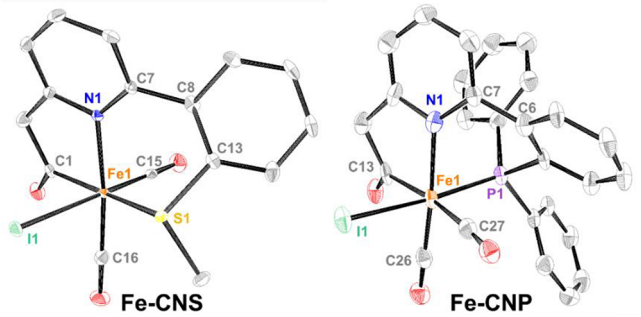

Figure 1. ORTEP diagram (50% thermal ellipsoids) of **Fe-CNS** (left) and **Fe-CNP** (right) exhibiting the *mer*-CNS or *fac*-CNP donor orientations, respectively. Hydrogen atoms are omitted for clarity. Color scheme: carbon (gray); nitrogen (blue); oxygen (red); sulfur (yellow); iron (orange); iodine (green); phosphorus (purple).

the position *trans* to the pyridine N, similar to the Hmd active site. However, the second carbonyl in each case is differentially located: *trans* to the iodide in **Fe-CNS**, and *trans* to the acyl-C donor in **Fe-CNP**. Each of the Fe−C(≡O) bond distances is approximately 1.77 Å, with the notable exception for the CO *trans* to the acyl moiety in **Fe-CNP**, which is nearly 0.1 Å longer (1.876(11) Å, Table 1). This is indicative of the strong σ-donor strength of the acyl-carbanion donor. The Fe−C_{acyl} bond distances for **Fe-CNS** and **Fe-CNP** are not drastically different (1.945(5) and 1.974(10) Å, respectively). Regarding **Fe-CNP**, a literature search reveals that the average distance a Fe−C_{acyl} bond with a *trans* CO is roughly 1.976 Å,[9,28,29,38,39] which is consistent with the value of **Fe-CNP** (1.974(10) Å). The Fe−I distances for both complexes are nearly identical: 2.6958(7) and 2.6980(17) Å for **Fe-CNS** and **Fe-CNP**, respectively.

In **Fe-CNS**, the N_{py}−Fe−C_{acyl} ferracycle angle is 85.19(17)° (Table 1). The aryl unit coupled at the *ortho* position on the pyridine ring is twisted out of plane by −41.2(7)°, primarily due to the steric hindrance between the hydrogen atoms on the pyridine and aryl rings *ortho* to the coupling site. This "flipped up" aryl group directs the thioether S to ligate to Fe center *trans* to the acyl moiety, thus affording the *mer* coordination motif. In contrast, the *ortho* aryl unit of the **CNP** ligand rotates in the opposite direction, characterized by a +38.9(13)° torsion angle. This allows the bulkier −PPh_2 moiety (versus −SMe) to occupy the site *trans* to iodide, rather than *cis* to iodide as in **Fe-CNS**.

The unexpected and spontaneous facial ligation of CNP can be explained by closely examining and comparing both steric and electronic effects on the Fe-acyl complexes. In both complexes, the coordination of the acyl C, pyridine N, iodide,

DOI: 10.1021/acs.inorgchem.9b01530
Inorg. Chem. 2019, 58, 12689−12699

Table 1. Selected Bond Lengths and Bond Angle Comparison between Fe-CNS and Fe-CNP

selected bond lengths (Å)			selected bond angles (deg)		
	Fe-CNS	Fe-CNP		Fe-CNS	Fe-CNP
$Fe-N_{py}$	2.031(4)	2.038(8)	$N_{py}-Fe-C_{acyl}$	85.19(17)	82.9(4)
$Fe-C_{acyl}$	1.945(5)	1.974(10)	$N_{py}-Fe-S/P$	*S*	*P*
				87.80(11)	79.1(2)
Fe−S/P	*S*	*P*	$N_{py}-C_{py}-C_{Ph}-C_{Ph'}$	−41.2(7)	38.9(13)
	2.3396(14)	2.202(3)			
Fe−CO	*trans-iodide*	*trans-acyl*			
	1.772(5)	1.876(11)	ligand binding	meridional (pincer-type)	facial
$Fe-CO_{trans-py}$	1.768(5)	1.774(11)	*trans* to acyl?	SMe	CO
Fe−I	2.6958(7)	2.6980(17)	*trans* to N^{py}?	CO	CO

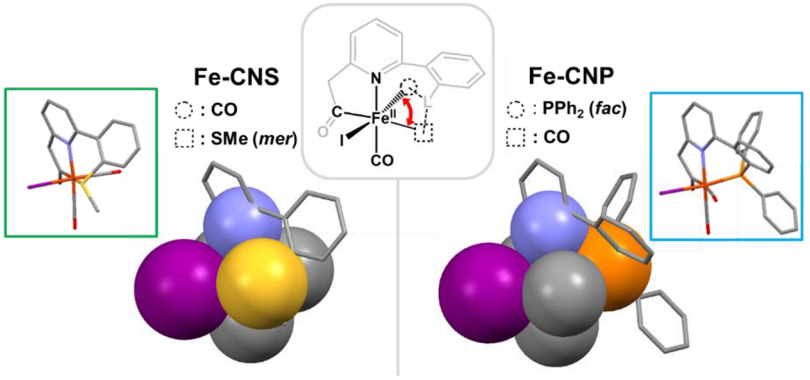

Figure 2. Structures of **Fe-CNS** and **Fe-CNP**, respectively, showing only the six donor atoms in space-filling model. Each inset represents the capped-sticks model of the larger structure at the same angle. Color scheme: carbon (gray); nitrogen (blue); iodine (dark magenta); sulfur (yellow); phosphorus (orange). Hydrogen atoms are omitted for clarity.

Scheme 4. Deprotonation of Fe-CNS or Fe-CNP with a Bulky Phenolate Base[a]

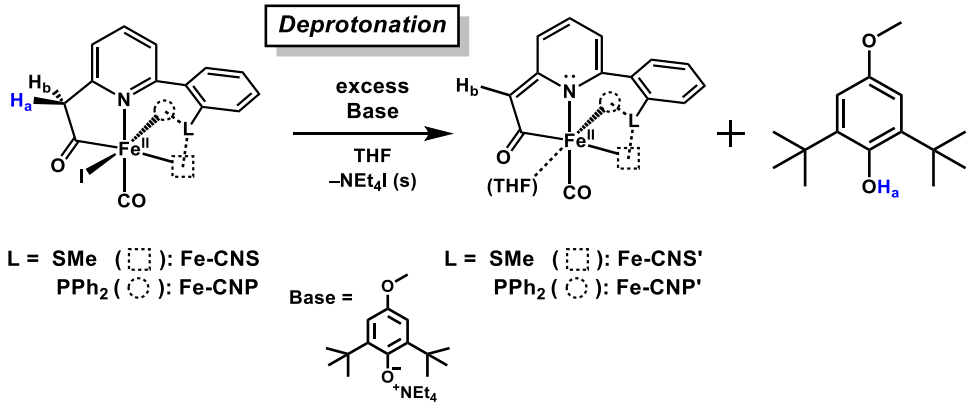

[a]The hollow wedged bond for one carbonyl group represents the position either *trans* from iodide (**Fe-CNS**) or *trans* from acyl (**Fe-CNP**).

and $CO_{trans-py}$ remains unchanged. Only two sites, those *trans* to iodide and *trans* to acyl (represented as dotted circle and dotted square in Figure 2, respectively) are occupied by different donors—namely, the second CO and either SMe or PPh_2. Also, space-filling models of both complexes reveal that the iodide is the bulkiest donor atom (radius: 206 pm) among the six; iodide is also larger than the combined CO ligand. Therefore, iodide will preferentially occupy the least crowded coordination site (complete space-filling models: Figure S2). For **Fe-CNS**, the second bulkiest donor is the SMe unit, while in **Fe-CNP** it is PPh_2 moiety. Comparing −SMe and $-PPh_2$, the former has only one "short" arm (methyl), which can easily be deflected away from the bulky iodide without changing the coordination site of the −SMe donor. On the other hand, $-PPh_2$ has two bulky substituents. Therefore, the bulky phosphine moiety cannot occupy the position *cis* to the bulkiest donor atom, iodide. Incidentally, the "flexibility" of the *ortho*-aryl linkage facilitates binding of the $-PPh_2$ unit *trans* to the iodide, while retaining unperturbed Fe−P bond metrics (2.202(3) Å); the facial CNP ligation is the final result.

Deeper inspection of the donor strengths of −SMe versus $-PPh_2$ also provides insight into the geometric properties of the complexes. Among the **CNS** and **CNP** donor sets, the *σ*-donor strength is ordered as follows: acyl-C > $-PPh_2$ > N_{py} > −SMe. Thus, the position *trans* from the acyl-C would be the most labile site due to its strong *trans* influence, thus dissuading the coordination of another strong *σ*-donor (such as $-PPh_2$). However, in case of **CNS**, the −SMe unit is a weak *σ*-donor not unlike the weakly bound H_2O molecule *trans* from acyl in the active site. Indeed, all of the previously reported

DOI: 10.1021/acs.inorgchem.9b01530
Inorg. Chem. 2019, 58, 12689−12699

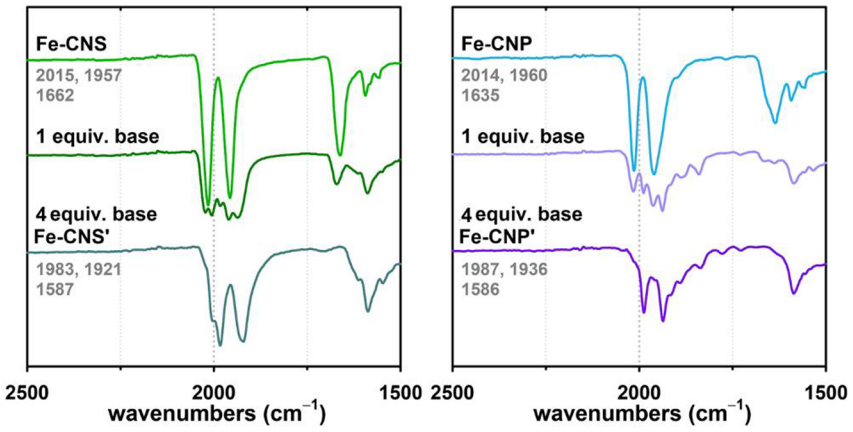

Figure 3. Infrared spectra of **Fe-CNS** (left) and **Fe-CNP** (right) deprotonation via bulky phenolate. Note that more than one equivalent of base is required for a complete deprotonation to **Fe-CNS′** or **Fe-CNP′**.

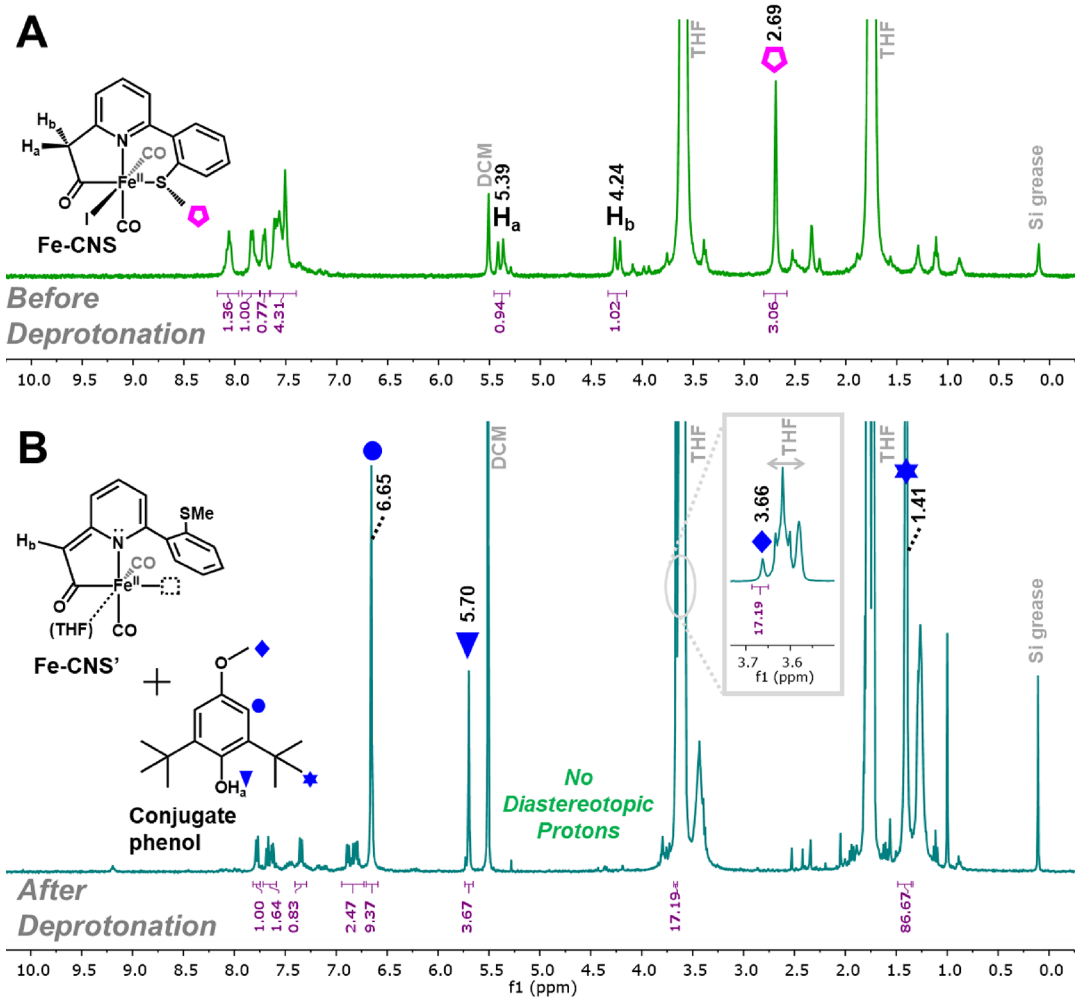

Figure 4. (A) ^{1}H NMR spectrum of **Fe-CNS** in d^8-THF. (B) ^{1}H NMR spectrum of deprotonated species **Fe-CNS′** and conjugate phenol + phenolate in d^8-THF.

iron-acyl-phosphine complexes[38−41] exhibit non-chelating phosphine ligand(s) at *cis* site(s). Similarly, all examples of iron-*carbamoyl* complexes that contain non-chelating phosphine ligands exhibit *cis*-phosphine(s), except for one case of a *trans* PMe_3 unit.[36,42] All of these data are consistent with the strong σ-donor effect of the acyl group, thus affording the *cis*-PPh_2 binding motif (and consequently, *fac*-CNP).

Reactivity Studies. *Deprotonation.* In related non-biomimetic work on iron(II) pincers, it has been established that heterolytic cleavage of H_2 occurs via metal−ligand cooperation that utilizes the conjugate base of acidic methylene or amide linkers in the ligand framework.[16] These conjugate bases are "dearomatized" due to the presence of a pyridinate anion (rather than pyridine) in the central position.

DOI: 10.1021/acs.inorgchem.9b01530
Inorg. Chem. 2019, 58, 12689−12699

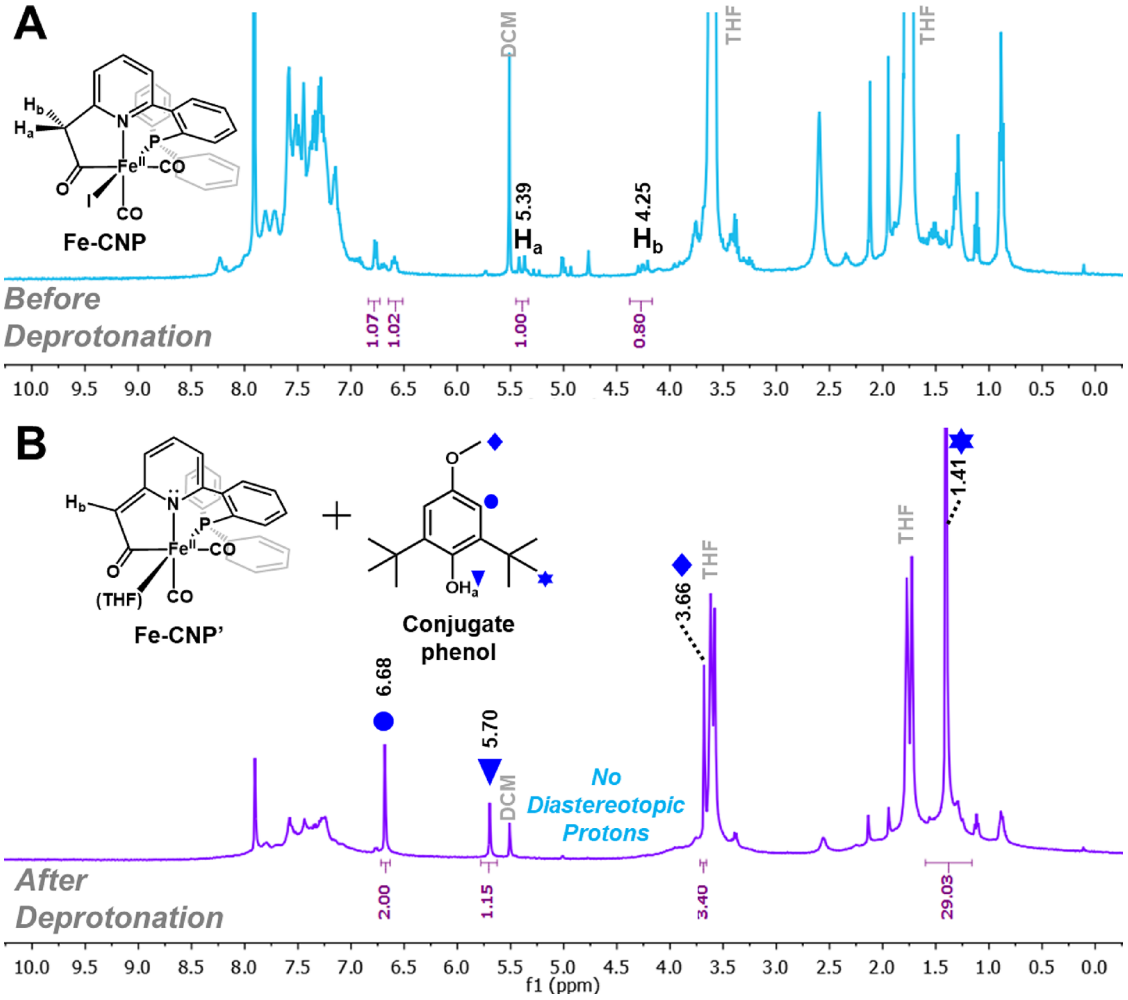

Figure 5. (A) ^{1}H NMR spectrum of **Fe-CNP** in d^8-THF. (B) ^{1}H NMR spectrum of deprotonated species **Fe-CNP′** and conjugate phenol + phenolate in d^8-THF.

In our biomimetic system, we found that the methylene linker protons serve an analogous role (Scheme 4).

Up to 4 equiv of base were required for a complete conversion of **Fe-CNS** to **Fe-CNS′**. The progress was monitored by infrared spectroscopy, showing a clear transition of the carbonyl stretches {2015, 1957} → {1983, 1921 cm^{-1}} as well as the acyl stretch (1662 → 1587 cm^{-1}) (Figure 3, left). Under similar conditions, deprotonation of a methylene proton of **Fe-CNP** yielded the dearomatized species **Fe-CNP′**, exhibiting red shift of the carbonyls {2014, 1960} → {1987, 1936 cm^{-1}} and the acyl (1635 → 1586 cm^{-1}) stretches in infrared spectrum (Figure 3, right). To confirm the acid/base nature of this transformation, attempts were made to regenerate the parent complex, **Fe-CNS**, by adding a proton source. Addition of 2,6-lutidinium bromide to **Fe-CNS′** did result in a blue shift of the carbonyl stretches {1983,1921} → {2002,1933 cm^{-1}} as expected (Figure S3), similar to **Fe-CNS**; however, the acyl stretch near 1665 cm^{-1} was only partially recovered. We also attempted to abstract iodide from **Fe-CNS** and **Fe-CNP** using either Na[BAr^F] or $AgBF_4$, in both the presence and absence of PPh_3: both reactions resulted in the loss of all CO, indicating the decomposition of the complexes.

The methylene protons in both iron−acyl complexes are diastereotopic—their chemical environment is quite different, resulting in two doublets in the ^{1}H NMR spectrum at 5.46 and 3.86 ppm for **Fe-CNS** in C_6D_6 (H_a and H_b, respectively; Figure S4A, top) and 5.79 and 4.94 ppm for **Fe-CNP** (Figure S4A, bottom). Comparing the structures of the two complexes, the chemical environments of the "front-side" protons adjacent to the iodide remain relatively similar, compared with distinct chemical environments of the "back-side" protons (adjacent to CO versus −PPh_2 in **Fe-CNS** versus **Fe-CNP**). The similar chemical shifts of 5.46 (**Fe-CNS**) and 5.79 (**Fe-CNP**) support the assignment of the downfield diastereotopic resonance to be H_a in both cases. The more deshielded nature of H_a indicates more susceptibility to deprotonation, and thus H_a is likely the acidic proton in the reactivity studies detailed below.

Reactivity studies required the use of THF or d^8-THF versus C_6D_6 as a coordinating solvent and for improved solubility of reagents. Treatment of **Fe-CNS** (^{1}H NMR spectrum, Figure 4A) with a bulky phenolate base (NEt_4^+ salt of 2,6-di-*tert*-butyl-4-methoxyphenolate) results in the disappearance of the diastereotopic resonances, indicating the formation of the dearomatized species **Fe-CNS′** (Figure 4B), analogous to the dearomatized iron-pyridinate species observed by Milstein and Kirchner.[16−21,43] As a result, the conjugate acid phenol is observed (δ OH: 5.70 ppm), and $NEt_4I_{(s)}$ is formed as precipitate. It is noted that an excess of the conjugate phenol (see assigned resonances in Figure 4B) remains observable due to the requirement for ∼4 equiv of phenolate to drive complete

DOI: 10.1021/acs.inorgchem.9b01530
Inorg. Chem. 2019, 58, 12689−12699

deprotonation (see IR section above, Figure 3, left). Lastly, the disappearance of the $-S(CH_3)$ resonance at 2.69 ppm suggests deligation of the sulfur donor due to the (now) dianionic ligand framework.

Similarly, as noted in the IR section (Figure 3, right), **Fe-CNP** also requires ~4 equiv of base to complete deprotonation. After treatment of **Fe-CNP** with the phenolate base, the diastereotopic protons (5.39 and 4.25 ppm in d^8-THF, Figure 5A) are no longer observed, and the resonances from the conjugate phenol emerge (Figure 5B).

D_2 Activation. The deprotonated species **Fe-CNS′** was then placed under 5 atm of D_2, and the reaction was monitored by ^{2}H NMR spectroscopy (Figure 6). A new resonance at 5.39

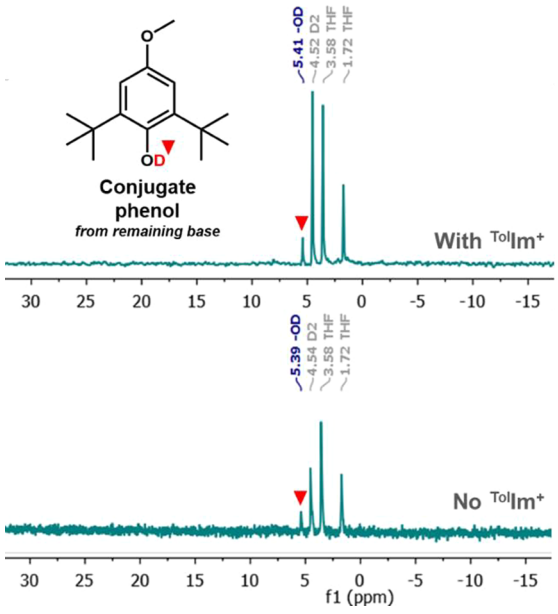

Figure 6. ^{2}H NMR spectra of D_2 activation by **Fe-CNS′** with or without the presence of substrate (^{Tol}Im$^+$) in THF, exhibiting an −OD signal of the conjugate phenol at 5.41 and 5.39 ppm, respectively.

ppm was observed within 30 min, which was assigned as the conjugate phenol−OD resonance (D^+, confirmed via isolation of the authentic phenol−OD species from CD_3OD);[34] no Fe−D resonance (D^-) was observed (e.g., 0 to −30 ppm). Nonetheless, the observation of the D^+ resonance indicates activation of D_2 via heterolysis by the **Fe-CNS** system. It is also notable in the ^{2}H NMR spectra that the ligand "basic site" is not deuterated during successful D_2 heterolysis, indicating that the methine carbon is not directly involved in D_2 activation.

A recent result from our group demonstrates that a bulky Lewis acid substrate (putative hydride acceptor) can be employed to stabilize and detect iron-hydride species in ^{2}H NMR experiments[34] or serve as a hydride-accepting substrate.[35] Therefore, the same reaction was performed in the presence of the model substrate ^{Tol}Im[BAr^F], a bulky imidazolium salt that mimics the role of methenyl-H_4MPT$^+$ in the enzyme's H_2 activation process. However, a nearly identical ^{2}H NMR spectrum was obtained in this case (δ −OD = 5.41 ppm; no Fe−D resonance observed), indicating that the ^{Tol}Im$^+$ substrate (a) does not impede H_2 heterolysis, (b) does not aid in stabilizing the implicit iron-deuteride intermediate, and (c) does not serve as a hydride acceptor in this system.

For the deprotonated phosphine congener **Fe-CNP′**, the analogous reaction with D_2 (7 atm, ^{2}H NMR analysis) does not result in a phenol−OD resonance (D^+); again, no Fe−D resonance was detected (Figure S6). This phenol-OD resonance has served as an obligate marker for D_2 heterolysis in all systems studied in our laboratory.[34,35] Indeed, following D_2 exposure, both the NMR spectra (^{1}H and ^{31}P) as well as IR analysis indicate that the unaltered **Fe-CNP′** remains the only detectable species; that is, no decomposition or methylene resonance (^{1}H or ^{2}H) is observed. We do note the presence of one minor peak in the ^{2}H spectrum near 7.8 ppm; however, based on the absence of ^{13}C{^{2}H} coupling in the ^{13}C NMR spectrum, we have been unable to identify this feature. Nonetheless, we similarly attempted to detect hydride transfer from D_2 to the ^{Tol}Im$^+$ substrate—unsurprisingly to no avail.

DISCUSSION

Fe-CNS versus Fe-CNP Reactivity. We postulate that the reason for the lack of D_2 activation in **Fe-CNP′** is due to the "blocking" of the coordination site *trans* to the acyl unit by the CO ligand. We have demonstrated the requirement for an open site *trans* to acyl in several other systems, including those supported by an anthracene scaffold that uniformly enforces a *fac*-CNS coordination motif with the solvent/H_2 binding site *trans* to the acyl unit.[34,35] This generates an apparent paradox with the **Fe-CNS** case, wherein the *trans* site is also "blocked" by the thioether-S donor. However, recent studies have indicated the potential hemilability of thioether-S in related systems. It is notable that in the enzyme site, one presumed role of the strongly σ donating, acyl carbanion is to labilize the weakly bound water to enable H_2 binding via Kubas interaction. We did demonstrate through IR spectroscopy in both coordinating (THF) and noncoordinating solvents (DCE, FPh) that the Fe−S bond remains intact in the **Fe-CNS** starting complex. It is likely, however, that upon generating another negative charge in the ligand frame (dearomatized pyridine anion), the sulfur deligates from the iron center. Ultimately, we propose the mechanistic cycle illustrated in Schemes 5 and 6, which is the only model consistent with all of our observations. In the case of **Fe-CNP**/**Fe-CNP′**, the consistent ligation of the CO ligand *trans* to the acyl unit blocks H_2 binding and activation, despite the generation of a basic site on the ligand frame.

Relevance to Enzyme. It is evident that the indispensable factor that dictates reactivity toward H_2 is the presence of an open coordination site *trans* to the organometallic acyl unit. It is likely that the presence of a pendant base is also required (methenyl-acyl in our work; pyridonate in enzyme). However, due to the hemilabile thioether in the **Fe-CNS** system, we are unable to unambiguously differentiate these two effects.

Regarding the pendant base postulate, the emerging mechanism for the enzyme is that this role is fulfilled by the pyridone moiety (rather than the Cys-S as in [NiFe], or azadithiolate in [FeFe]). However, our system lacks the truly biomimetic and anionic pyridonate donor and instead employs the neutral pyridine as a substitute. We wish to highlight the limited implication of the deprotonated methylene(acyl) *pyridine* unit observed in our system, versus the methylene-(acyl)*pyridone* unit in the enzyme: Due to the pre-existing anionic charge in the enzyme's pyridonate heterocycle, we strongly contend that the methylene(acyl) pK_a would be biologically inaccessible; its deprotonation would require the generation of a *di*-anionic pyridone—unlikely. Therefore, *we*

DOI: 10.1021/acs.inorgchem.9b01530
Inorg. Chem. 2019, 58, 12689−12699

Scheme 5. Summary of Mechanistic Understanding of the Parameters Leading (or Blocking) H_2 Activation in the Present Fe-CNS and Fe-CNP Systems

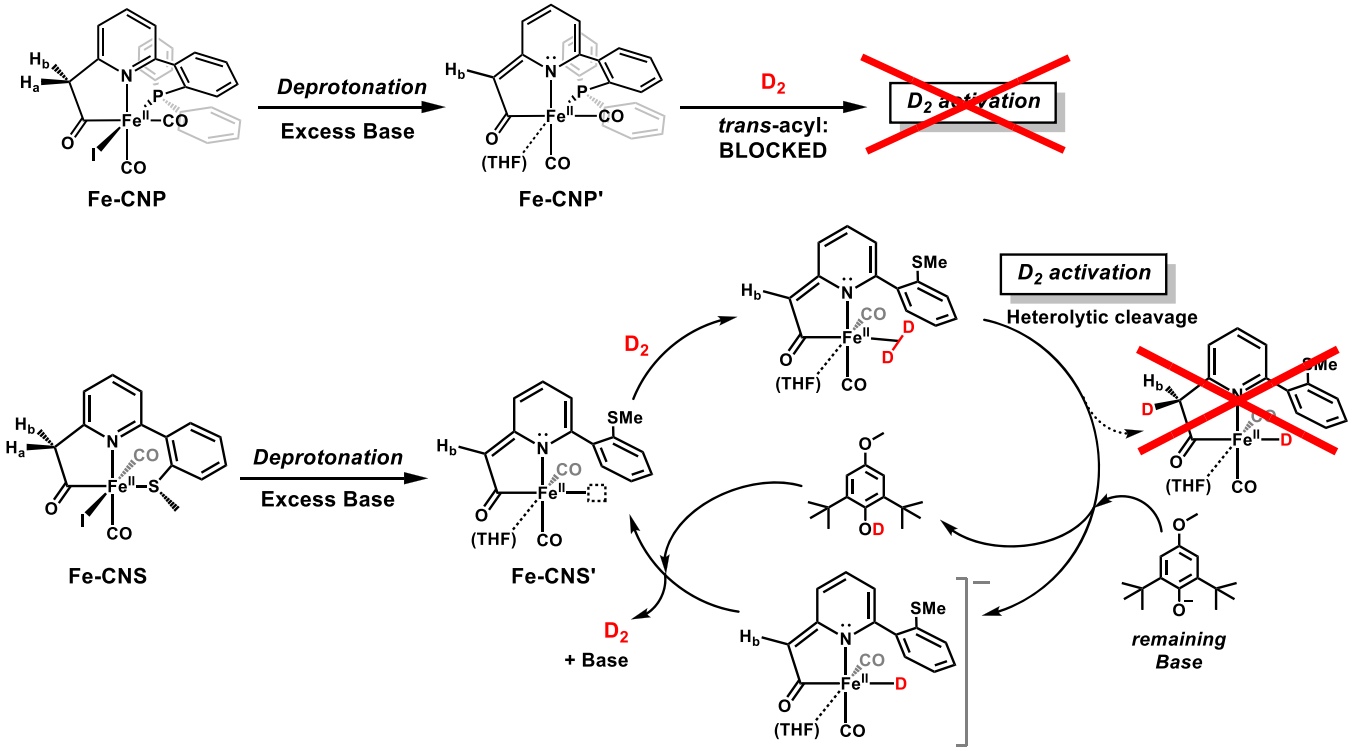

Scheme 6. Difference in Methylene Reactivity (Acidity) between the Enzyme Active Site (Top) and Present Fe-CNS/Fe-CNP Systems

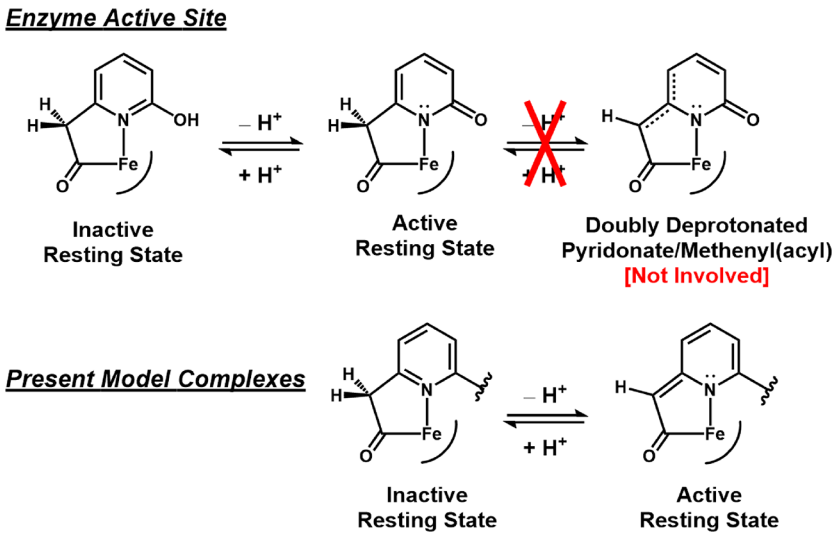

do not claim that the methylene(acyl) → methenyl(acyl) interconversion is an active mechanism in the enzyme. Rather, we contend that the present system demonstrates the important utility of a pendant base in the vicinity of the iron center to drive H_2 heterolysis.

CONCLUSION

In summary, we were able to directly compare the electronic and steric effects on the binding mode of thioether versus triphenylphosphine moiety in Fe-acyl system by designing two pincer ligand precursors, **CNS**^{Pre} and **CNP**^{Pre}. The **CNS** ligand adopted the expected *mer*-CNS motif, while the **CNP** adopted an unexpected *fac*-CNP motif due to the bulkier and more strongly σ-donating $-PPh_2$ unit (does not prefer to bind *trans* to the acyl carbanion). The reactivity studies are summarized as follows:

(1) Both **Fe-CNS** and **Fe-CNP** undergo facile methylene-(acyl) deprotonation that generates a dearomatized pyridinate similar to that reported by Milstein, Kirchner, and others.

(2) In all cases, the **Fe-CNP** system exhibits a "blocked" coordination site *trans* to the organometallic acyl unit, which precludes H_2 binding and activation.

DOI: 10.1021/acs.inorgchem.9b01530
Inorg. Chem. 2019, 58, 12689−12699

(3) In contrast, deprotonation of the **Fe-CNS** system generates an open coordination site *trans* to acyl, which enables H_2 activation. This highlights the key importance of the geometric location of the H_2 binding site as *trans* from the acyl unit to promote H_2 binding and heterolysis.
(4) However, neither a stable iron-hydride species nor hydride transfer to a biomimetic substrate is observed in **Fe-CNS** system. We suspect that the anionic nature of the proposed Fe−H intermediates result in their instabilities, thereby precluding spectroscopic detection.
(5) The methylene(acyl) motif occurs in both the present systems and the enzyme. In **Fe-CNS** and **Fe-CNP**, it serves as a convenient means to investigate the role of "pendant base" in a model system.
(6) However, due to the already anionic pyridone in the active site (versus neutral pyridine in this model system), *it is not claimed that the methylene(acyl) → methenyl(acyl) conversion occurs in the enzyme*. The endogenous pyridone-O likely serves the role of "pendant base" in the active site.

EXPERIMENTAL SECTION

Materials and Methods. $Fe(CO)_5$ and $Pd(PPh_3)_4$ were purchased from Strem Chemicals; 2-bromo-6-methylpyridine and $Pd(PPh_3)_2Cl_2$, from Oakwood Chemicals; 2-(methylthio)phenyl boronic acid, from Boron Molecular and Matrix Scientific; 2-bromophenylboronic acid from Combi Blocks, Inc.; I_2 and $ClPPh_2$, from Acros Organics; 1.6 M *n*BuLi in hexanes and D_2 (99.8%), from Sigma-Aldrich; K_2CO_3, from Fisher Scientific; aluminum oxide (neutral, Brockmann I, 50−200 μm, 60 Å), from Acros Organics; silica (SiliaFlash Irregular Silica Gels, 40−63 μm, 40 Å), from SiliCycle. The solvents dimethoxyethane (DME), ethyl acetate (EA), and 1,4-dioxane were purchased from Fisher Scientific and used without further purification. The solvents diethyl ether (Et_2O), dichloromethane (DCM), chloroform, tetrahydrofuran (THF), and pentane were procured from Fisher Scientific and dried over alumina columns using a Pure Process Technology solvent purification system and stored over 3 Å molecular sieves until use. The deuterated solvent $CDCl_3$ was purchased from Cambridge Isotopes and used as received. Imidazolium (Im^+)[44] and the bulky phenolate base were synthesized following literature procedures.

Physical Methods. Infrared spectra were recorded on a Bruker Alpha spectrometer equipped with a diamond ATR crystal. ^1H and ^{31}P NMR spectra were collected using Varian DirecDrive 400 MHz, while ^2H NMR spectra were collected using Varian DirectDrive 600 MHz. Elemental analyses were performed by Midwest Micro Lab.

Syntheses of Ligand Precursors and Complexes. ***CNS^{Pre}*** *(2-Methyl-6-(2-(methylthio)phenyl)pyridine, $C_{13}H_{13}NS$).* A Suzuki coupling of 2-bromo-6-methylpyridine (4.0 g, 23 mmol) with 2-(methylthio)phenyl boronic acid (5.9 g, 35 mmol) was performed using 1 M K_2CO_3 (35 mmol) and *trans*-$Pd(PPh_3)_2Cl_2$ (0.816 g, 1.2 mmol, 5 mol %) in 100 mL of DME. The slurry was heated at 85 °C for 24 h in a pressure vessel. The organic layer was collected by ethyl acetate (EA) extractions (3 × 100 mL) and dried over Na_2SO_4. Purification via column chromatography (EA:Hex = 1:8) afforded the product as a pale yellow oil. Yield: 3.4 g (67%). ^1H NMR (CDCl3, δ in ppm): 7.64 (t, J = 7.7 Hz, 1H), 7.42 (ddd, J = 7.6, 1.5, 0.6 Hz, 1H), 7.38−7.30 (m, 3H), 7.22 (ddd, J = 7.5, 6.7, 1.9, 1H), 7.13 (dtd, J = 7.6, 1.0, 0.4, 1H), 2.63 (s, 3H), 2.39 (s, 3H). HRMS (+ESI): m/z calcd for $C_{13}H_{13}NS$ (M), 215.08; found, $(M + H)^+$ 216.0845.

Fe-CNS *[(CNS)Fe(CO)$_2$(I)].* The **CNS^{Pre}** (0.400 g, 1.86 mmol) was dissolved in 10 mL of Et_2O and degassed by freeze−pump−thaw method. Then it was cooled to −10 °C for the addition of *n*BuLi (1.6 M in hexanes, 1.86 mmol). After the addition, the reaction was stirred at rt for 45 min. After the formation of an orange slurry, a prechilled Et_2O solution (3 mL) of $Fe(CO)_5$ (250 μL, 1.86 mmol) was added dropwise at −78 °C. The reaction mixture was stirred for about 1.5 h and allowed to warm to −25 °C, then recooled to −78 °C for oxidation. Under dark conditions, the prechilled Et_2O solution (7 mL) of I_2 (0.212 g, 1.67 mmol) was added dropwise into the stirred solution via cannula transfer and kept at −78 °C for 2 h. A yellow−brown precipitate was isolated using an air-free filter tube and dried under N_2. Yield: 0.528 g (59.3%). A DCM solution of the crude product was then filtered through neutral alumina and layered with pentane at −25 °C to give X-ray quality crystals (red−brown needles). ^1H NMR (C_6D_6, δ in ppm): 7.36 (s, 1H), 6.96 (s, 1H), 6.88−6.78 (m, 2H), 6.72 (t, J = 7.8 Hz,1H), 6.61 (d, J = 7.7 Hz, 1H), 6.26 (d, J = 7.8 Hz, 1H), 5.46 (d, J = 20.5 Hz, 1H), 3.86 (d, J = 20.4 Hz, 1H), 2.00 (s, 3H). ^1H NMR (d^8-THF, δ in ppm): 8.07 (m, 1H), 7.83 (d, J = 8.1 Hz, 1H), 7.71 (d, J = 7.5 Hz, 1H), 7.65−7.40 (m, 4H), 5.39 (d, J = 20.4 Hz, 1H), 4.24 (d, J = 20.4 Hz, 1H), 2.69 (s, 3H). IR bands (cm^{-1}): 2032 ($\nu_{C\equiv O}$ vs), 1962 ($\nu_{C\equiv O}$ vs), 1662 ($\nu_{C=O}$ vs), 1583, 1572, 1474 (s), 1449, 1438 (s), 760, 744 (s). Elemental analysis for calcd (**Fe-CNS** with residual solvents: 0.1 equiv DCM and 0.2 equiv pentane): C 40.75, H 2.92, N 2.78; found: C 40.90, H 2.80, N 2.41. CCDC deposition no.: 1590122.

2-(2-Bromophenyl)-6-methylpyridine ($C_{12}H_{10}BrN$). A Suzuki coupling of 2-bromo-6-methylpyridine (3.27 g, 19.0 mmol) with 2-bromophenylboronic acid (4.20 g, 20.9 mmol, 1.1 equiv) was performed using K_2CO_3 (2.89 g, 20.9 mmol, 1.1 equiv) and $Pd(PPh_3)_4$ (0.769 g, 0.66 mmol, 3.5 mol %) in a 1,4-dioxane:H_2O (3:1) mixture. The slurry was refluxed for 24 h. The organic layer was collected by EA extractions (3 × 100 mL) and dried over Na_2SO_4. Purification via column chromatography (EA:Hex = 1:8) afforded the product as pale yellow oil. Yield: 3.89 g (83%). ^1H NMR ($CDCl_3$, δ in ppm): 7.67−7.57 (m, 2H), 7.50 (dd, J = 7.6, 1.8 Hz, 1H), 7.40−7.33 (m, 2H), 7.20 (dddd, J = 7.5, 1.8, 0.5 Hz, 1H), 7.13 (dp, J = 7.7, 0.3 Hz, 1H), 2.62 (s, 3H). HRMS (+ESI): m/z calcd for $C_{12}H_{10}BrN$ (M), 247.00, 249.00; found, $(M + H)^+$ 248.0071, 250.0051.

CNP^{Pre} *(2-(2-(Diphenylphosphaneyl)phenyl)-6-methylpyridine, $C_{24}H_{20}NP$).* [The synthetic conditions were modified from the work of Speiser et al.[37]] Note: A rigorous air-free handling technique is required to isolate this product as the free phosphine (avoiding phosphine oxide). A solution of *n*BuLi (1.6 M in hexanes, 16 mmol) was added dropwise into a freeze−pump−thawed solution of 2-(2-bromophenyl)-6-methylpyridine (3.97 g, 16 mmol) in THF at −78 °C. After stirring the solution at the same temperature for 1 h, $ClPPh_2$ (16 mmol) was added dropwise via syringe and allowed to warm to rt overnight. Degassed H_2O was added via syringe, followed by successive air-free Et_2O extractions using cannula transfers. The organic layer was transferred to a N_2-purged Schlenk flask containing Na_2SO_4 via cannula and stirred for 30 min. The dried solution was then cannula transferred to a new Schlenk flask, and the volume was reduced under vacuum until a white powder formed. The resulting yellow supernatant (impurities) was transferred into a separate Schlenk flask via cannula, and the remaining white powder (product) was washed several times with cold Et_2O, then dried under N_2. Storage of the supernatant and washes at −20 °C for 2 d afforded large colorless blocks suitable for X-ray diffraction. Yield: 2.94 g (52%). ^1H NMR ($CDCl_3$, δ in ppm): 7.59 (ddd, J = 7.6, 4.3, 1.3 Hz, 1H), 7.49 (t, J = 7.7 Hz, 1H), 7.39 (td, J = 7.5, 1.4 Hz, 1H), 7.34−7.18 (m, 12H), 7.04 (dddd, J = 7.7, 3.9, 1.4, 0.5 Hz, 1H), 6.97 (d, J = 7.8 Hz, 1H), 2.27 (s, 3H). ^{31}P NMR ($CDCl_3$, δ in ppm): −10.9 (s). CCDC deposition no.: 1590145. HRMS (+ESI): m/z calcd for $C_{24}H_{20}NP$ (M), 353.13; found, $(M + H)^+$ 354.1413.

Fe-CNP *[(CNP)Fe(CO)$_2$(I)].* The **CNP^{Pre}** (0.500 g, 1.42 mmol) was dissolved in 15 mL of Et_2O and degassed by freeze−pump−thaw. The solution was cooled to −10 °C for the addition of nBuLi (1.6 M in hexanes, 1.42 mmol). After the addition, the reaction was stirred at rt for 45 min. After the formation of an orange slurry, a prechilled Et_2O solution (3 mL) of $Fe(CO)_5$ (191 μL, 1.42 mmol) was added dropwise at −78 °C. The reaction mixture was stirred for about 1.5 h and allowed to warm to −25 °C, then again cooled to −78 °C for oxidation. Under dark conditions, the prechilled Et_2O solution (7 mL) of I_2 (0.162 g, 1.27 mmol) was added dropwise into the stirring solution and kept at −78 °C for 2 h. A yellow−brown precipitate was

DOI: 10.1021/acs.inorgchem.9b01530
Inorg. Chem. 2019, 58, 12689−12699

isolated using an air-free filter tube and, then, dried under N_2. Yield: 0.615 g (77.9%). The crude product was purified by dissolving in DCM and loaded on a short alumina (neutral) column in an N_2 atmosphere glovebox; the products were eluted using a series of solvents of increasing polarity (DCM → $CHCl_3$ → THF). The final elution with THF produced a yellow solution, from which the product was collected via crystallization (vapor diffusion of pentane into the THF solution at rt). Small orange−brown clusters of X-ray quality crystals were generated after ∼10 days. ^{1}H NMR (C_6D_6, δ in ppm): 7.7−6.4 (m, 17H), 5.79 (d, J = 20.2 Hz, 1H), 4.94 (d, J = 20.8 Hz, 1H). ^{1}H NMR (d^8-THF, δ in ppm): 8.0−7.0 (m, 15H), 6.77 (d, J = 7.5 Hz, 1H), 6.59 (t, J = 9.0 Hz, 1H), 5.39 (d, J = 20.2 Hz, 1H), 4.25 (dd, J = 20.9, 14.1 Hz, 1H). ^{31}P NMR (C_6D_6, δ in ppm): 79.9 (s). IR bands (cm^{-1}): 2011 ($\nu_{C\equiv O}$ vs), 1974 ($\nu_{C\equiv O}$ vs), 1637 ($\nu_{C=O}$ vs), 1590, 1473 (s), 1427, 1092 (s), 979, 765 (s), 742 (s), 691 (vs), 602 (vs), 565, 543, 509 (s). Elemental analysis for $C_{27}H_{19}FeINO_3P$, calcd: C 52.38, H 3.09, N 2.26; found: C 52.48, H 3.32, N 2.14. CCDC deposition no.: 1590123.

Reactivity Studies. In a glovebox under an N_2 atmosphere, a small portion of iron−acyl complex (approximately 10 mg) was dissolved in 1 mL of THF at rt. Up to approximately 4 equiv of bulky phenolate base was added until all three CO stretches were determined to be completely red-shifted via IR spectroscopy. For experiments with the substrate, 1 equiv of Im[BAr^F] was added to the solution at this point. The solution was then filtered through celite and transferred to a high-pressure J-Y NMR tube. The tube was removed from the glovebox and its headspace was filled with 5 atm of D_2 gas. Gentle mixing was provided by slow, periodic inversion (Stuart Rotator SB2) over the course of 30−60 min, after which the reaction was complete (no further changes were observed in the ^{2}H NMR spectrum at ∼24 h).

■ ASSOCIATED CONTENT

Supporting Information

The Supporting Information is available free of charge on the ACS Publications website at DOI: 10.1021/acs.inorgchem.9b01530.

X-ray data collection and refinement details, ORTEP diagram, space-filling models, IR and NMR (^{1}H, ^{31}P, and ^{2}H) spectra (PDF)

Accession Codes

CCDC 1590122−1590123 and 1590145 contain the supplementary crystallographic data for this paper. These data can be obtained free of charge via www.ccdc.cam.ac.uk/data_request/cif, or by emailing data_request@ccdc.cam.ac.uk, or by contacting The Cambridge Crystallographic Data Centre, 12 Union Road, Cambridge CB2 1EZ, UK; fax: +44 1223 336033.

■ AUTHOR INFORMATION

Corresponding Author

*Email: mrose@cm.utexas.edu.

ORCID

Michael J. Rose: 0000-0002-6960-6639

Notes

The authors declare no competing financial interest.

■ ACKNOWLEDGMENTS

This research was supported by the National Science Foundation (NSF CHE-1808311) and the Welch Foundation (F-1822). The authors are grateful to Dr Vince Lynch for assistance with X-ray data collection and structure refinement, as well as Dr Steve Sorey and Dr Garrett Blake for assistance in acquiring and analyzing NMR spectra. The authors also thank Spencer Kerns and Zhu-Lin Xie for assistance in preparing D_2 reactivity experiments.

■ REFERENCES

(1) Lubitz, W.; Ogata, H.; Rüdiger, O.; Reijerse, E. Hydrogenases. *Chem. Rev.* **2014**, *114* (8), 4081−4148.

(2) Shima, S.; Pilak, O.; Vogt, S.; Schick, M.; Stagni, M. S.; Meyer-Klaucke, W.; Warkentin, E.; Thauer, R. K.; Ermler, U. The Crystal Structure of [Fe]-Hydrogenase Reveals the Geometry of the Active Site. *Science* **2008**, *321*, 572−575.

(3) Shima, S.; Thauer, R. K. A third type of hydrogenase catalyzing H_2 activation. *Chem. Rec.* **2007**, *7* (1), 37−46.

(4) Huang, G.; Wagner, T.; Wodrich, M. D.; Ataka, K.; Bill, E.; Ermler, U.; Hu, X.; Shima, S. The atomic-resolution crystal structure of activated [Fe]-hydrogenase. *Nat. Catal.* **2019**, *2*, 537−543.

(5) Hiromoto, T.; Ataka, K.; Pilak, O.; Vogt, S.; Stagni, M. S.; Meyer-Klaucke, W.; Warkentin, E.; Thauer, R. K.; Shima, S.; Ermler, U. The crystal structure of C176A mutated [Fe]-hydrogenase suggests an acyl-iron ligation in the active site iron complex. *FEBS Lett.* **2009**, *583* (3), 585−590.

(6) Hiromoto, T.; Warkentin, E.; Moll, J.; Ermler, U.; Shima, S. The Crystal Structure of an [Fe]-Hydrogenase-Substrate Complex Reveals the Framework for H_2 Activation. *Angew. Chem., Int. Ed.* **2009**, *48* (35), 6457−6460.

(7) Shima, S.; Vogt, S.; Göbels, A.; Bill, E. Iron-chromophore circular dichroism of [Fe]-hydrogenase: The conformational change required for H_2 activation. *Angew. Chem., Int. Ed.* **2010**, *49* (51), 9917−9921.

(8) Turrell, P. J.; Wright, J. A.; Peck, J. N. T.; Oganesyan, V. S.; Pickett, C. J. The third hydrogenase: A ferracyclic carbamoyl with close structural analogy to the active site of Hmd. *Angew. Chem., Int. Ed.* **2010**, *49* (41), 7508−7511.

(9) Chen, D.; Scopelliti, R.; Hu, X. A five-coordinate iron center in the active site of [Fe]-hydrogenase: Hints from a model study. *Angew. Chem., Int. Ed.* **2011**, *50* (25), 5671−5673.

(10) Wodrich, M. D.; Hu, X. Electronic elements governing the binding of small molecules to a [Fe]-hydrogenase mimic. *Eur. J. Inorg. Chem.* **2013**, *2013* (22−23), 3993−3999.

(11) Hu, B.; Chen, D.; Hu, X. Synthesis and reactivity of mononuclear iron models of [Fe]-hydrogenase that contain an acylmethylpyridinol ligand. *Chem. - Eur. J.* **2014**, *20* (6), 1677−1682.

(12) Chen, D.; Scopelliti, R.; Hu, X. [Fe]-hydrogenase models featuring acylmethylpyridinyl ligands. *Angew. Chem., Int. Ed.* **2010**, *49* (41), 7512−7515.

(13) Grützmacher, H. Cooperating Ligands in Catalysis. *Angew. Chem., Int. Ed.* **2008**, *47*, 1814−1818.

(14) Van Der Vlugt, J. I.; Reek, J. N. H. Neutral tridentate PNP ligands and their hybrid analogues: Versatile non-innocent scaffolds for homogeneous catalysis. *Angew. Chem., Int. Ed.* **2009**, *48* (47), 8832−8846.

(15) Crabtree, R. H. Multifunctional ligands in transition metal catalysis. *New J. Chem.* **2011**, *35* (1), 18−23.

(16) Bauer, G.; Kirchner, K. A. Well-defined bifunctional iron catalysts for the hydrogenation of ketones: Iron, the new ruthenium. *Angew. Chem., Int. Ed.* **2011**, *50* (26), 5798−5800.

(17) Langer, R.; Leitus, G.; Ben-David, Y.; Milstein, D. Efficient Hydrogenation of Ketones Catalyzed by an Iron Pincer Complex. *Angew. Chem., Int. Ed.* **2011**, *50* (9), 2120−2124.

(18) Zell, T.; Ben-David, Y.; Milstein, D. Unprecedented iron-catalyzed ester hydrogenation. Mild, selective, and efficient hydrogenation of trifluoroacetic esters to alcohols catalyzed by an iron pincer complex. *Angew. Chem., Int. Ed.* **2014**, *53* (18), 4685−4689.

(19) Zell, T.; Milstein, D. Hydrogenation and Dehydrogenation Iron Pincer Catalysts Capable of Metal−Ligand Cooperation by Aromatization/Dearomatization. *Acc. Chem. Res.* **2015**, *48*, 1979−1994.

(20) Garg, J. A.; Chakraborty, S.; Ben-David, Y.; Milstein, D. Unprecedented iron-catalyzed selective hydrogenation of activated

DOI: 10.1021/acs.inorgchem.9b01530
Inorg. Chem. 2019, 58, 12689−12699

amides to amines and alcohols. *Chem. Commun.* **2016**, *52* (30), 5285−5288.
(21) Bichler, B.; Holzhacker, C.; Stöger, B.; Puchberger, M.; Veiros, L. F.; Kirchner, K. A. Heterolytic cleavage of dihydrogen by an iron(II) PNP pincer complex via metal-ligand cooperation. *Organometallics* **2013**, *32* (15), 4114−4121.
(22) Bichler, B.; Glatz, M.; Stöger, B.; Mereiter, K.; Veiros, L. F.; Kirchner, K. A. An iron(II) complex featuring (3) and labile (2)-bound PNP pincer ligands - striking differences between CH_2 and NH spacers. *Dalton Trans.* **2014**, *43* (39), 14517−14519.
(23) Gorgas, N.; Stöger, B.; Veiros, L. F.; Pittenauer, E.; Allmaier, G.; Kirchner, K. A. Efficient Hydrogenation of Ketones and Aldehydes Catalyzed by Well-Defined Iron(II) PNP Pincer Complexes: Evidence for an Insertion Mechanism. *Organometallics* **2014**, *33*, 6905−6914.
(24) He, L.-P.; Chen, T.; Gong, D.; Lai, Z.; Huang, K.-W. Enhanced reactivities toward amines by introducing an imine arm to the pincer ligand: Direct coupling of two amines to form an imine without oxidant. *Organometallics* **2012**, *31* (14), 5208−5211.
(25) Chen, T.; He, L.-P.; Gong, D.; Yang, L.; Miao, X.; Eppinger, J.; Huang, K.-W. Ruthenium(II) pincer complexes with oxazoline arms for efficient transfer hydrogenation reactions. *Tetrahedron Lett.* **2012**, *53* (33), 4409−4412.
(26) Min, S.; Rasul, S.; Li, H.; Grills, D. C.; Takanabe, K.; Li, L. J.; Huang, K.-W. Electrocatalytic Reduction of Carbon Dioxide with a Well-Defined PN^3-Ru Pincer Complex. *ChemPlusChem* **2016**, *81* (2), 166−171.
(27) Song, L.-C.; Xie, Z.-J.; Wang, M.-M.; Zhao, G.-Y.; Song, H.-B. Biomimetic models for the active site of [Fe] hydrogenase featuring an acylmethyl(hydroxymethyl)pyridine ligand. *Inorg. Chem.* **2012**, *51* (14), 7466−7468.
(28) Song, L.-C.; Zhao, G.-Y.; Xie, Z.-J.; Zhang, J.-W. A novel acylmethylpyridinol ligand containing dinuclear iron complex closely related to [Fe]-hydrogenase. *Organometallics* **2013**, *32* (9), 2509−2512.
(29) Song, L.-C.; Hu, F.-Q.; Zhao, G.-Y.; Zhang, J.-W.; Zhang, W.-W. Several new [Fe]hydrogenase model complexes with a single Fe center ligated to an acylmethyl(hydroxymethyl)pyridine or acylmethyl(hydroxy)pyridine ligand. *Organometallics* **2014**, *33* (22), 6614−6622.
(30) Chen, D.; Scopelliti, R.; Hu, X. Reversible protonation of a thiolate ligand in an [Fe]-hydrogenase model complex. *Angew. Chem., Int. Ed.* **2012**, *51* (8), 1919−1921.
(31) Shima, S.; Chen, D.; Xu, T.; Wodrich, M. D.; Fujishiro, T.; Schultz, K. M.; Kahnt, J.; Ataka, K.; Hu, X. Reconstitution of [Fe]-hydrogenase using model complexes. *Nat. Chem.* **2015**, *7* (12), 995−1002.
(32) Bart, S. C.; Lobkovsky, E.; Chirik, P. J. Preparation and Molecular and Electronic Structures of Iron(0) Dinitrogen and Silane Complexes and Their Application to Catalytic Hydrogenation and Hydrosilation. *J. Am. Chem. Soc.* **2004**, *126* (42), 13794−13807.
(33) Lagaditis, P. O.; Sues, P. E.; Sonnenberg, J. F.; Wan, K. Y.; Lough, A. J.; Morris, R. H. Iron(II) Complexes Containing Unsymmetrical P−N−P′ Pincer Ligands for the Catalytic Asymmetric Hydrogenation of Ketones and Imines. *J. Am. Chem. Soc.* **2014**, *136* (4), 1367−1380.
(34) Seo, J.; Manes, T. A.; Rose, M. J. Structural and functional synthetic model of mono-iron hydrogenase featuring an anthracene scaffold. *Nat. Chem.* **2017**, *9*, 552−557.
(35) Kerns, S. A.; Magtaan, A.-C.; Vong, P. R.; Rose, M. J. Functional Hydride Transfer by a Thiolate-Containing Model of Mono-Iron Hydrogenase featuring an Anthracene Scaffold. *Angew. Chem., Int. Ed.* **2018**, *57*, 2855−2858.
(36) Durgaprasad, G.; Xie, Z.-L.; Rose, M. J. Iron Hydride Detection and Intramolecular Hydride Transfer in a Synthetic Model of Mono-Iron Hydrogenase with a CNS Chelate. *Inorg. Chem.* **2016**, *55* (2), 386−389.
(37) Speiser, F.; Braunstein, P.; Saussine, L. Nickel Complexes Bearing New P,N-Phosphinopyridine Ligands for the Catalytic Oligomerization of Ethylene. *Organometallics* **2004**, *23* (11), 2633−2640.
(38) Xu, T.; Yin, C. J. M.; Wodrich, M. D.; Mazza, S.; Schultz, K. M.; Scopelliti, R.; Hu, X. A Functional Model of [Fe]-Hydrogenase. *J. Am. Chem. Soc.* **2016**, *138* (10), 3270−3273.
(39) Song, L.; Xu, K.; Han, X.; Zhang, J. Synthetic and Structural Studies of 2-Acylmethyl-6-R- Difunctionalized Pyridine Ligand-Containing Iron Complexes Related to [Fe]-Hydrogenase. *Inorg. Chem.* **2016**, *55*, 1258−1269.
(40) Hu, B.; Chen, X.; Gong, D.; Cui, W.; Yang, X.; Chen, D. Reversible CO Dissociation of Tricarbonyl Iodide [Fe]-Hydrogenase Models Ligating Acylmethylpyridyl Ligands. *Organometallics* **2016**, *35*, 2993−2998.
(41) Zhao, D.; Xu, Y.; Guo, Y.; Song, H.; Tang, L. Synthesis and reactivity of (pyrazol-1-yl) acyl iron complexes. *J. Organomet. Chem.* **2015**, *791*, 303−310.
(42) Turrell, P. J.; Hill, A. D.; Ibrahim, S. K.; Wright, J. A.; Pickett, C. J. Ferracyclic carbamoyl complexes related to the active site of [Fe]-hydrogenase. *Dalton Trans.* **2013**, *42*, 8140−8146.
(43) Butschke, B.; Feller, M.; Diskin-Posner, Y.; Milstein, D. Ketone hydrogenation catalyzed by a new iron(II)−PNN complex. *Catal. Sci. Technol.* **2016**, *6* (12), 4428−4437.
(44) Kalz, K. F.; Brinkmeier, A.; Dechert, S.; Mata, R. A.; Meyer, F. Functional model for the [Fe] hydrogenase inspired by the frustrated lewis pair concept. *J. Am. Chem. Soc.* **2014**, *136* (47), 16626−16634.

DOI: 10.1021/acs.inorgchem.9b01530
Inorg. Chem. 2019, 58, 12689−12699